Research Article

Nano Biomed Eng

Labeling MCF-7 Cell Line with Interleukin-6/Calcium Phosphate Nanoparticles

Seda Genç, Nelisa Türkoğlu✉

Department of Molecular Biology and Genetics, Yıldız Technical University, Istanbul, Turkey

✉ Corresponding author. E-mail: nelisalacin@gmail.com

Abstract

In recent years, nanoparticle systems have been frequently used as non-viral carriers for the treatment of genetically based diseases and cancer. However, the conjugate formation should be optimized by selecting a suitable carrier for the transport of each genetic material desired to be transported to the target cell. A suitable conjugate should be created by taking into account the size and zeta potential electrical characteristics of the cargo being transported. Nanocarrier systems can protect and package genetic material. Calcium phosphate nanoparticles (CaP NPs) with unique advantages have been a promising approach for *in vitro* and *in vivo* gene transfers. However, the biggest challenge of the CaP NPs is their unreducible size. In this study, CaP NPs were synthesized via the co-precipitation method using two stabilizing agents separately: magnesium nitrate and sodium citrate. The transfection efficiency of nanoparticles obtained by using sodium citrate in the MCF-7 cell line was observed to be more effective compared to magnesium nitrate-containing nanoparticles. The nanoparticles with a size of (248.1 ± 54) nm (polydispersity index (PDI), 0.3) and zeta potential of (-13.3 ± 2.8) mV were synthesized. The morphological properties of the particles were determined by scanning electron microscopy (SEM) and atomic force microscopy (AFM). Cytotoxicity of nanoparticles was performed by 3-(4,5-dimethylthiazol-2-yl)-2,5-diphenyltetrazolium bromide (MTT) analysis using L929 mouse fibroblast cells. In the study, both CaP/plasmid DNA conjugation and naked plasmid DNA were transferred to MCF-7 cells, and the gene expression efficiency was determined by fluorescent microscopy via green fluorescent protein (GFP) expression. Gene expression efficiencies were determined as 24% ($\pm$1.7%) for naked pDNA and 76% ($\pm$2.3%) for CaP-conjugated pDNA, respectively.

Keywords: immunotherapy; interleukin (IL)-6; calcium phosphate nanoparticle; gene transfer

Introduction

Cancer immunotherapy focuses on developing an anti-cancer response by using the patient's immune system to compete with cancer cells. Tumor-associated immune cells have a critical role in tumorigenesis. Immune cells in the tumor microenvironment (TME) have a role in tumor formation and tumor growth. The tumor-associated immune cells may function on destroying a tumor, leading to apoptosis, or support the tumor and ensure its proliferation [1]. Cytokines are small protein groups that play roles in the growth and differentiation of cells, especially for regulation of the immune system and inflammation. Certain cytokines activate or suppress the T-cell response against cancer

cells. In the literature, the effects of interleukins and interferons on cancer treatment continue to be investigated. It has been reported that the interleukin (IL)-6 cytokine, which has a critical role in various cellular events, activates the apoptotic pathway by increasing the level in cancer cells [2, 3]. Therefore, IL-6 cytokine was used in this study.

Gene therapy is a breakthrough strategy that focuses on the regulation of gene regions responsible for inherited disorders and diseases such as cancer [4]. Effective gene transfer strategies applied in gene therapy highly depend on the development of the carrier systems called "vectors". The vector system enables the transfer of the therapeutic gene to the target cell. Naked DNA can not enter the cell alone and not maintain its activation for a long time without preservation. In addition, naked DNA can be degraded by various enzymes on the way to reaching the nucleus after passing through the cell membrane. The transfection of target genes into cells via carrier vectors is efficient compared to naked DNA [5, 6].

Viral and non-viral vectors provide gene transfer of biological agents such as DNA, RNA, and siRNA to target cells. Both approaches have advantages and disadvantages [7–9]. The nanoparticle systems, belonging to the non-viral group and with advantages such as high reliability, high gene carrying capacity, biocompatibility, low immunogenic response, and low toxicity, have been used quite frequently for several decades [10–12].

Nanoparticle systems, i.e., nanocarriers, have become more popular with the development of nanotechnology. Certain nanoparticles can easily penetrate and pass through the cell membrane. It has been reported in various studies that nanoparticles can be used in clinical treatment, gene therapy, monitoring of intracellular biological processes, and high-efficiency transfection [5, 13–15]. Nanoparticles (NPs) are also promising for cancer immunotherapy, determination of cancer cells, and tumor destruction. NPs have advantages in protecting bioactive molecules such as DNA, RNA, and drugs against fragmentation inside and outside the cell. Thus, we have the opportunity to manipulate target cells via them. NPs have become the most preferred vectors for gene transfer in the recent literature [12].

Calcium phosphate (CaP) NPs were first used in gene transfer in 1973 by Graham and Van Der Eb [16].

CaP is an inorganic biomaterial found in mammalian hard tissues such as bones and teeth. In addition, calcium and phosphate components are biodegradable and biocompatible as they occur naturally in the body. CaP NPs can carry molecules containing target genes [17, 18]. They have a higher loading capacity compared to other inorganic vectors, and their surface is filled with a very dense charge due to the Ca^{2+} and PO_4^{3-} molecules charges and thus are competent to bind with various organic molecules [19].

The phosphate group in the DNA structure makes the DNA a negatively charged molecule. The positively charged calcium ions of the CaP NPs interact with the phosphate in the DNA backbone with a strong affinity [20]. It has also stated that divalent metal cations such as Ca^{2+}, Mg^{2+}, Mn^{2+}, and Ba^{2+} are used for the synthesis of CaP NPs from ionic complexes with the helical phosphates of DNA. The complexes are transported across the cell membrane via endocytosis [21].

The size of the CaP NPs greatly affects the transfection efficiency. A major drawback of them is that they tend to grow over time via agglomeration and end up with a decrease in transfection efficiency. Parameters such as the concentration of calcium and phosphate ions and pH are critical to minimizing nanoparticle aggregation [22]. Besides, Mg ion utilization to balance the nanoparticle mineralization and obtain smaller-sized particles seems as an option [23]. In other words, the inhibitory effect of Mg ion on particle growth can be explained by the creation of a distorted atomic structure in hydroxyapatite. Thus, it reduces the growth rate of particles. Another ion used to provide stabilization was sodium (Na). Calcium and sodium have similar ionic radii and therefore Na ions can potentially occupy a cationic position. It is reported in the literature that Na ions move to calcium places and form OH- spaces. When Ca ion is replaced by Na ion, it causes a change in the size of the apatite crystal. The substitution of Na ions with Ca ions and the deprotonation of phosphate groups adversely affect aggregation. Consequently, the presence of Na ions in solution inhibits the formation of large aggregates [24].

CaP NPs have been shown to have an outstanding place in clinical research and biomedical applications such as transfection of therapeutic biomolecules, gene silencing, and drug delivery. In particular, the development of CaP NPs carrying anticancer

therapeutics has become a focus of increasing interest [18].

In this study, we aimed to label a target cancer cell line with IL-6 cytokine. We transfected the plasmid DNA encoding IL-6 via the CaP NPs to the MCF-7 cancer cell line and evaluated the transfection efficiency. In the literature, Mg ion has been used to reduce the size of CaP NPs. In this study, we report that particles containing Na ion are slightly smaller in size than particles containing Mg ion.

Materials and Methods

Materials

Chemical reagents calcium nitrate, diammonium hydrogen phosphate, magnesium nitrate, and sodium citrate were purchased from Sigma-Aldrich, USA. Trypsin-ethylenediamine tetra acetic acid (Trypsin-EDTA), fetal bovine serum (FBS), and Dulbecco's Modified Eagle Medium (DMEM F-12) were obtained from Biological Industries (Israel) for use in cell culture studies. The breast cancer cell line (MCF-7) was purchased from the FMD Institute Turkey. The pEGFP N1-IL6 plasmid was an Addgene (plasmid 111933) purchased.

Methods

Amplification and purification of plasmid encoding IL-6 and green fluorescent protein (GFP)

In this study, the plasmid (Addgene Plasmid 111933: pEGFP N1-IL6) encoding IL-6, kanamycin resistance, and GFP was used. The plasmid was introduced to a competent *E.coli* bacteria to be amplified. The bacterial culture was inoculated in Petri dishes (100 μg of kanamycin per 1 mL of LB agar), then incubated overnight at 37 °C. On the next day, the colonies were transferred to an LB medium (100 μg of kanamycin per 1 mL of broth). Colonies were incubated overnight at 37 °C and 400 r/min. Finally, the alkaline lysis, adsorption, washing, and desorption for the purification of plasmid DNA were performed following the kit protocol (Qiagen Inc®, Germany). The determination of concentration was performed by spectrophotometer considering the absorbance values of 260/280 nm.

Synthesis of CaP NPs

CaP NPs were synthesized via the precipitation method with some modifications [25]. Calcium nitrate, diammonium hydrogen phosphate, sodium citrate, and magnesium nitrate components were used separately as stabilizing agents. Two different nanoparticles were synthesized by using two different stabilizing agents: Na-CaP (the sodium-containing nanoparticle) and Mg-CaP (the magnesium-containing nanoparticle) to obtain small-sized nanoparticles. Calcium nitrate $Ca(NO_3)_2$, 25 mL of $4H_2O$ (9 mg/mL), and 25 mL of diammonium hydrogen phosphate $(NH_4)2HPO_4$ (2 mg/mL) was prepared in two separate beakers. The solutions were kept at 80 °C for 35 min. Then, calcium nitrate and diammonium hydrogen phosphate were mixed on a magnetic stirrer for 7 min at 60 °C. After this step, 50 mL of 3 mg/mL sodium citrate and magnesium nitrate components was slowly added to each solution for 6 min. The solutions were kept in the sonic probe (50% amplitude, pulse on for 4 s, pulse off for 2 s) for 15 min to ensure their homogenization. Then, the prepared solutions were transferred to the centrifuge tubes and centrifuged for 20 min (40 000 r/min at 20 °C). Following centrifugation, the supernatant was removed and the pellet containing nanoparticles was dissolved in distilled water and washed.

Characterization of CaP NPs

The average particle size, zeta potential, and polydispersity index (PDI) of the synthesized nanoparticle dispersions were determined by Zeta-sizer Device (Malvern Instruments Inc, UK). Determination of particle size and the zeta potential was carried out by the DLS method in distilled water at 25 °C. Scanning electron microscope (SEM) (Carl Zeiss, USA) and atomic force microscope (AFM) (Shimadzu SPM 9600, Japan) were used to determine their morphological properties. For the analyses, the nanoparticles were dried and then used. The structure of chemical bonds in the molecules forming the calcium phosphate nanoparticle and the determination of intramolecular functional groups were determined by Fourier transform infrared (FTIR) (Perkin Elmer Inc. USA).

Cytotoxicity of CaP NPs

In the study, the *in vitro* cytotoxicity of the CaP NPs on the L929 mouse fibroblast cell line (ATCC ® CRL-6364™) was determined by 3-(4,5-dimethylthiazol-2-yl)-2,5-diphenyltetrazolium bromide (MTT) analysis. Cells were seeded in a 96-well culture plate (10^5 cells per well). The plate was incubated at 37 °C and 5% CO_2 for 24 h. CaP NPs at different concentrations

(10, 20, 30, 40, and 50 μg/μL) were added to the wells. Then the medium containing nanoparticles was removed and 100 μL of MTT (5 mg/mL in medium) solution was added and icubated for 4 h. Finally, the MTT solution was discarded and 100 μL of dimethylsulfoxide (DMSO) was added to each well. Optic density was determined at 570 nm with an ELISA reader (Thermo Scientific Multiskan Go, USA).

Preparation and characterization of plasmid DNA/CaP NPs conjugate

Conjugates at different concentrations were prepared to ensure the stability of pDNA and CaP NPs. The conjugates were prepared by adding 1 μg of plasmid DNA solution to 40 μL of CaP solution (1 μg/μL), and then incubated for 30 min. The DNA purity was 1.9 at 260/280 nm. The size and zeta potential analyses of the obtained conjugates at 25 °C were characterized by Zeta-sizer.

Transfection of nanoparticle/DNA conjugate into MCF-7 cancer cell line

The MCF-7 cells were cultured with DMEM/F12 medium containing 10% FBS. 24 h before transfection, MCF-7 cells were seeded at 5×10^5 cells/mL in each well (6 well-plate) and incubated overnight at 37 °C and 5% CO_2. The serum-containing medium was replaced with serum-free DMEM/F-12 1 h before the transfection. Meanwhile, pDNA/nanoparticle transfection agents were prepared. pDNA/nanoparticle transfection agents were incubated at room temperature for approximately 1 h for the conjugate formation. Transfected cells were incubated at 37 °C and 5% CO_2 for 4 h. Then, the serum-free medium was replaced with DMEM/F-12 medium containing 10% FBS. Transfection efficiency was determined for 3 days using fluorescence microscopy via GFP expression of the plasmid in transfected cells. Cells were counted for 3 days and the calculation was made by averaging the values.

Results and Discussion

Characterization of CaP NPs

The size and zeta potential of the nanoparticles and pDNA/CaP NPs

The size, PDI, and zeta potential of the particles were determined by Zeta-sizer Nano ZS (Malvern Instruments, Malvern, UK) instrument. Two different nanoparticles were synthesized using ions that will stabilize the rapidly growing calcium phosphate nanoparticles. The size, PDI, and zeta potentials of Mg–CaP nanoparticles were found to be (365 ± 51) nm, 0.4, and (−21.8 ± 4.6) mV, respectively. The size, PDI, and zeta potentials of Na–CaP NPs were determined as (248.1 ± 54) nm, 0.3, and (−13.3 ± 2.8) mV, respectively (Table 1).

It has been observed that calcium phosphate NPs, which have similar zeta potential values with the studies in the literature, have a negative charge [26, 27]. Chowdhury et al. evaluated the CaP nanoparticles, with magnesium, for high gene expression in mammalian cells, in a time interval of 1–30 min and stated that their size distribution was increasing gradually [23]. Pedraza et al. have stated that the diameter of CaP particles varies up to 200 nm. They performed gene transfection successfully on the osteoblastic cell line by loading pDNA into the nanoparticles they synthesized [28]. Wu et al. reported that CaP particle sizes synthesized and coated with lipid molecules at different concentrations vary between 257.3 and 473.8 nm [29]. Similar to the method used in this study, Sokolova et al. synthesized calcium phosphate nanoparticles. They reported that agents such as magnesium and aluminum prevented the growth of nanoparticle size, and more stable particles were formed [17]. Welzel et al. synthesized calcium phosphate nanoparticles using the standard precipitation method. They succeeded in coating the nanoparticles with DNA and transfecting to human endothelial cells [30]. Sokolova et al. synthesized DNA functionalized calcium phosphate nanoparticles by the precipitation method. They transfected three cell lines (Hela, LTK, T-HUVEC) with plasmid DNA encoding GFP. They reported that the efficiency of transfection increased with nanoparticles formed a triple layer with DNA [31].

It is well-known calcium and +2 valence ions in the structure of CaP nanoparticles interact with phosphate groups of the DNA backbone. In the study, the size and zeta potential of pDNA/Na–CaP conjugate were (634.3 ± 90.4) nm and (−19.1 ± 7.3) mV, respectively. The size and zeta potential of pDNA/Mg–CaP conjugate were (815.1 ± 56.4) nm and (−29.3 ± 4.14) mV, respectively (Table 1). The results revealed that Na–CaP (the sodium-containing nanoparticle)

Table 1 Zeta potentials of CaP NPs and pDNA/CaP NPs

Nanoparticles	Size (nm)	Zeta potentials (mV)	Polydispersity index
Na-CaP	248.1 ± 54	−13.3 ± 2.8	0.3
Na-CaP/pDNA	634.3 ± 90.4	−19.1 ± 7.3	0.4
Mg-CaP	365 ± 51	−21.8 ± 4.6	0.4
Mg-CaP/pDNA	815.1 ± 56.4	−29.3 ± 4.14	0.5

was found to be smaller in dimension and more suitable for transfection and further studies.

The calcium phosphate nanoparticles' negative charge increases following interaction with DNA [19]. The zeta potentials of the Na–CaP NPs (40 μg/μL) conjugated with plasmid DNA at different concentrations (1, 2, 3, 4, 5, and 6 μg) were summarized in Table 2. It was determined that as the concentration of plasmid DNA increased, the negative charge of pDNA/CaP conjugate also increased in proportion. The results confirm that the conjugates formed with plasmid DNA interacted successfully with the nanoparticle under its purpose. Conjugate 1 was preferred for transfection studies from 6 conjugates prepared and given in Table 2. NP/plasmid DNA conjugates were prepared by adding 1 μg of plasmid DNA (0.33 μg/μL) to 40 μL of CaP NPs solution (1 μg/μL).

Morphological characterization of nanoparticles

The morphology of nanoparticles was determined by SEM (Fig. 1) and AFM (Fig. 2). It has been observed

the particles have a spherical shape and a single-size distribution. According to the analyzes with SEM and AFM, smaller dimensions were determined when compared to the dimensions determined by the DLS technique since the nanoparticles do not have a hydration layer (liquid phase) during SEM and AFM analyses because the NPs were analyzed following a lyophilization. In addition, we observed the arrangement of nanoparticles by obtaining two-dimensional (2D) and three-dimensional (3D) images, as well as the size distributions of nanoparticles by AFM analysis.

Hoo et al. performed the characterization of the nanoparticles in the range of 20–100 nm, using DLS and AFM analyses. They reported that AFM values were lower than DLS and nominal values [32]. When we examined the analysis, the images obtained were quite similar to the studies in the literature.

The chemical characterization of nanoparticles

FTIR analysis was performed to determine the

Table 2 Zeta potentials varying according to pDNA concentration

CaP–DNA conjugate	CaP (μg)	DNA (μg)	Zeta potentials (mV)	Polydispersity index
I	40	1	−19.1 ± 7.37	0.412
II	40	2	−23.8 ± 4.22	0.507
III	40	3	−24.9 ± 5.69	0.524
IV	40	4	−26.4 ± 6.11	0.627
V	40	5	−26.8 ± 5.75	0.695
VI	40	6	−27.8 ± 6.57	0.705

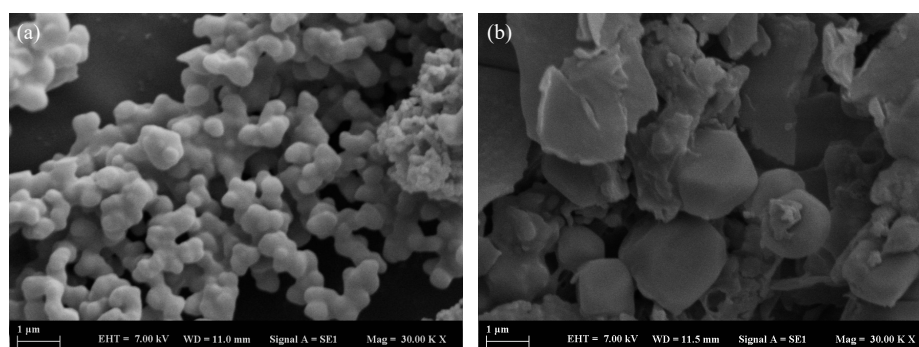**Fig. 1** SEM microphotographs of CaP NPs. (**a**) Image of Na-CaP NPs. (**b**) Image of Mg-CaP NPs.
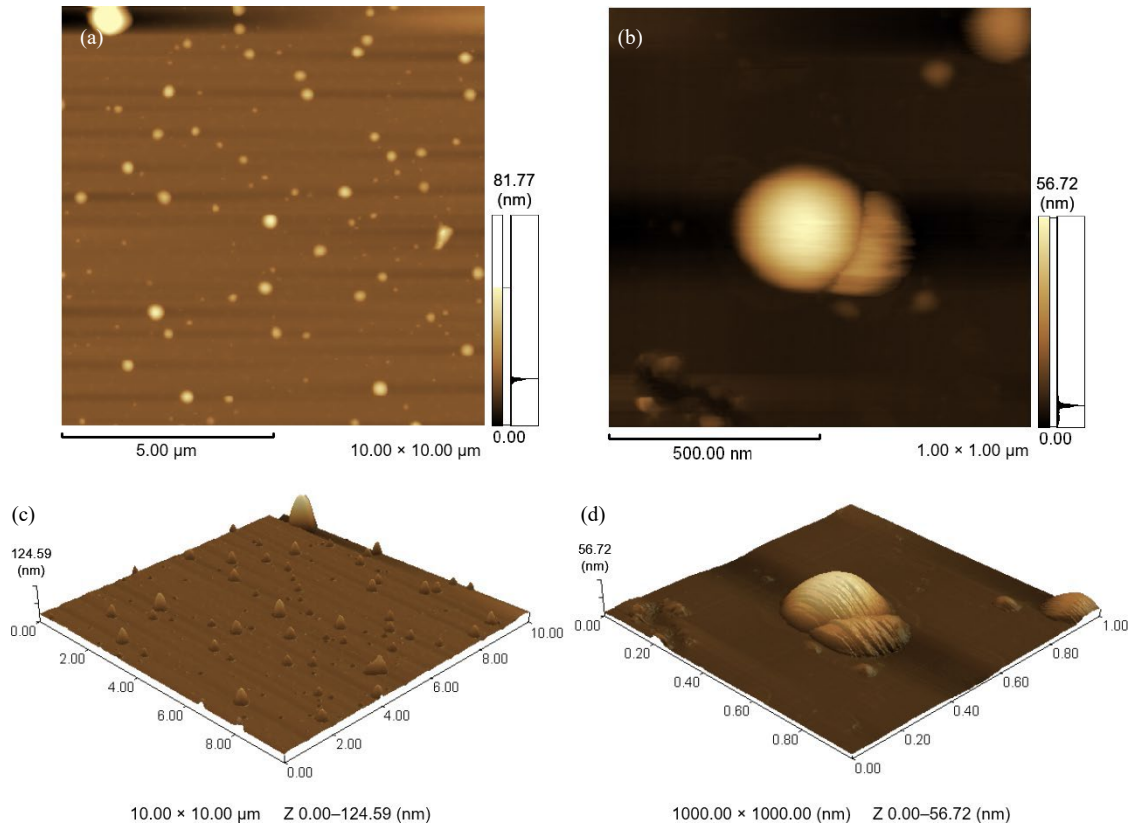
Fig. 2 AFM image of Na-CaP NPs (1 μm × 1 μm). (**a**) 2D view of 10 μm × 10 μm scan of calibrated spheres. (**b**) AFM image of a single sphere. 3D view of (**c**) 10 μm × 10 μm and (**d**) 1 μm × 1 μm scan of calibrated sphere.

presence of chemical bonds and functional groups in the structure of CaPs. Using the IR spectrum, the chemical bonds in the particles are as shown in Fig. 3. According to the IR spectrum, the bonds in the pure calcium nitrate chemical were the peaks near 3 409, 1 633, and 1 316 cm^{-1} are ─COOH, C═O, and C─H bonds, respectively. The characteristic peaks in the calcium nitrate salt were sharper and more pronounced than the peaks in the sodium citrate salt. The characteristic peaks in the diammonium

Fig. 3 FTIR spectrum of the chemicals used for the synthesis of CaPs and Ca/P NPs.

hydrogen phosphate structure were ─COOH, C═O, C─H, and P─O bonds that cause stretching of 3 211, 1 635, 1 434, and 1 043 cm^{-1}, respectively. According to the IR spectrum of the synthesized CaP NPs, values of 3 253, 1 580, 1 386, 1 022, and 843 cm^{-1} represent ─COOH, C═O, C─H, P─O, and C─H bonds, respectively. Phosphate groups in the Di-H-P structure represented the peaks of the nanoparticle.

Cytotoxicity of calcium phosphate nanoparticles

In vitro cytotoxicity of calcium phosphate nanoparticles was determined by MTT assay. The MTT assay was performed on the L929 fibroblast cell line. Nanoparticles were prepared and tested for 5 different concentrations (10, 20, 30, 40, and 50 μg/μL). 1% DMSO was used as positive control and DMEM F-12 medium was used as a negative control. The data obtained were shown in Fig. 4. The viability of cells was determined as 74.9% (±1.8%) for 10 μg/μL, 72.5% (±1.4%) for 20 μg/μL, 70% (±1.6%) for 30 μg/μL, 70.6% (±1.1%) for 40 μg/μL, and 65.1% (±2.3%) for 50 μg/μL. As shown in Fig. 4, it can be concluded that as the amount of nanoparticle increases, the toxicity increases. However, the

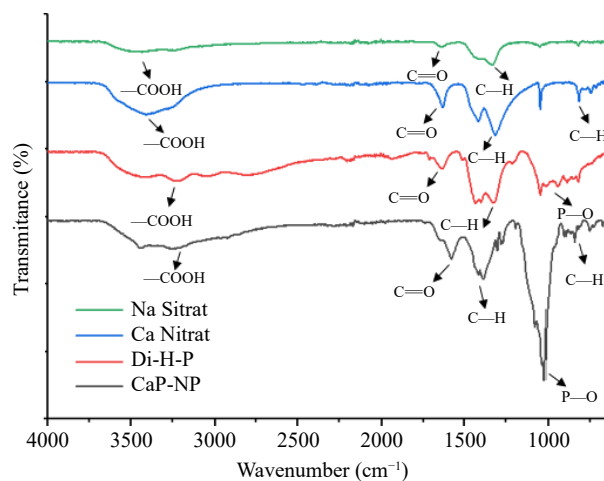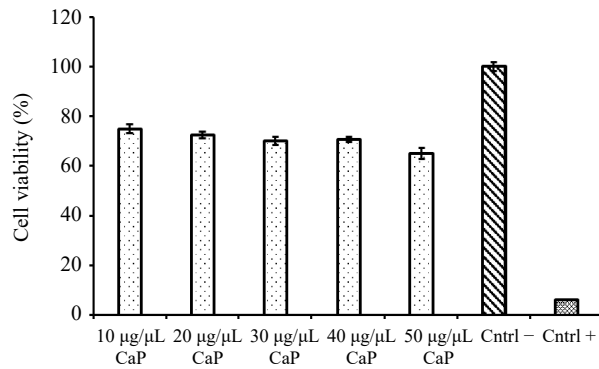**Fig. 4** The cell viability of fibroblast L929 following CaP interaction.

cytotoxic effect of the nanoparticles on the L929 cell line determined was tolerable for all concentrations, and cell viability was above 65% for five different concentration of NPs. In the literature, studies reported that calcium phosphate nanoparticles do not have a toxic effect on cells or that their cytotoxic effect is quite low [33, 34]. It has been reported that calcium phosphate nanoparticles prepared with additives such as silver and ammonium have a higher toxic effect [35].

Transfection of plasmid DNA/nanoparticle conjugate to MCF-7 cells and evaluation of transfection efficiency

In this study, transfection of plasmid DNA encoding IL-6 cytokine to MCF-7 cancer cell line was performed using a non-viral synthetic calcium phosphate nanoparticle. The transfection efficiency was evaluated. Transfection efficiency was determined by observing the green fluorescent light scattered by the expression of the GFP reporter gene for 3 days using a fluorescent microscope. Cell images showed that calcium phosphate nanoparticles carried plasmid DNA into MCF-7 cells in vitro. Phase-contrast and fluorescence images of transfected cells are shown in Fig. 5. In the study, the transfection efficiency of naked DNA and plasmid DNA conjugated with carrier vector was compared. Gene expression efficiencies were determined as 24% ($\pm$1.7%) for pDNA and 76% ($\pm$2.3%) for pDNA conjugated with CaP NPs, respectively. The transfection efficiency of the vector-directed DNA was significantly higher than the naked DNA. We have shown that transfection of therapeutic genes with CaP NPs to target cancer cells through nanoparticles is possible with this study, and we hope that cancer cells labeled with IL-6 can be easily recognized by the patient's immune system cells. We conclude that this study will pave the way for a new treatment approach in the field of cancer immunotherapy.
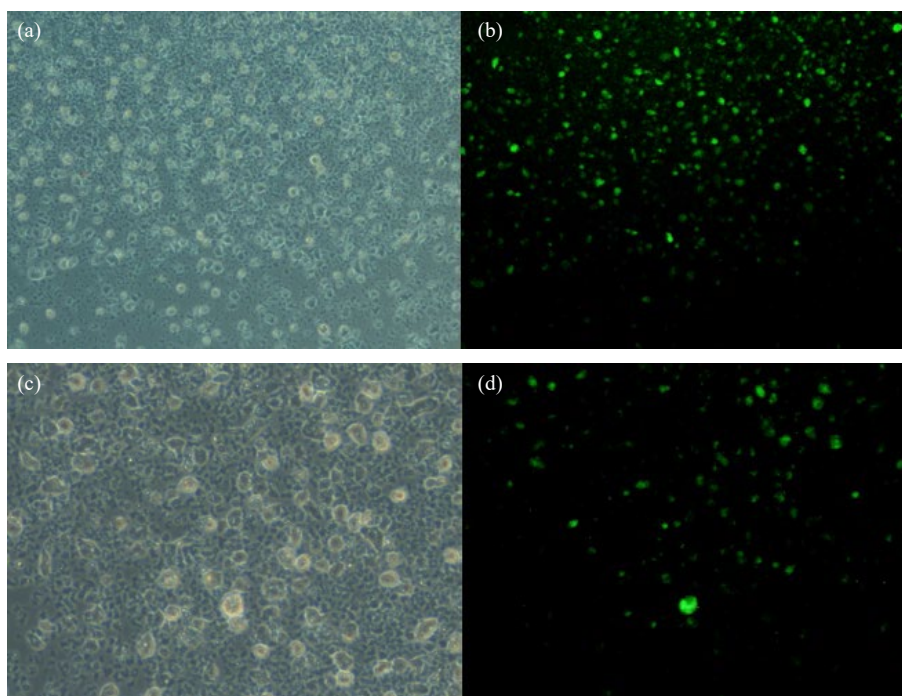

Fig. 5 Images of transfected MCF-7 cell line. (**a**) Phase contrast image transfected with CaP NP/pDNA. (**b**) Fluorescent image transfected with CaP NP/pDNA. (**c**) Phase contrast image transfected with naked plasmid DNA. (**d**) Fluorescent contrast image transfected with naked plasmid DNA.

Conclusion

In recent years, nanoparticle systems have been used *in vitro* and *in vivo* for the treatment of various diseases, especially cancer. CaP NPs have been one of the safest and most common systems used for this purpose. In cancer immunotherapy, targeted treatment modalities are possible by knocking out tumor cells. Cancer immunotherapy via nanoscale carrier vectors gained clinical success in therapeutic gene delivery.

Nanoparticles provide an advantage as a immune-stimulating agent system in the formation of anti-tumor responses. In addition, the delivery of naked plasmid DNA to cells reduces transfection efficiency due to intracellular degradation. Delivery of plasmid DNA to cells packaged with nanoparticles (synthesized by physical, chemical, and biological methods) increases transfection efficiency. In the study, CaP NPs, which are biocompatible, easier to manufacture, and significantly low toxic in comparison to other nanoparticles, were evaluated. Naked plasmid DNA and pDNA/nanoparticle conjugates were transfected to cancer cell lines and the transfection efficiency was determined. Gene expression efficiencies were determined as 76% (±2.3%) for pDNA conjugated with CaP. The synthesized nanoparticles successfully transferred pEGFP N1- and IL-6 plasmid DNA to the MCF-7 cell line. We aim to use the optimized IL-6/ calcium phosphate conjugates for future immunotherapy studies.

CRediT Author Statement

Seda Genç: Investigation, visualization, writing original draft, synthesis and characterization of CaP-nanoparticles, and cell culture studies. **Nelisa Türkoğlu:** Project administration, writing original draft, and cell culture studies.

Conflict of Interests

The authors declare that no competing interest exists.

Acknowledgments

References

[1] K.F. Goliwas, J.S. Deshane, C.A. Elmets, et al. Moving immune therapy forward targeting TME. *Physiological Reviews*, 2021, 101(2): 417−425. https://doi.org/10.1152/physrev.00008.2020

[2] C. Minichsdorfer, C. Wasinger, E. Sieczkowski, et al. Tocilizumab unmasks a stage-dependent interleukin-6 component in statin-induced apoptosis of metastatic melanoma cells. *Melanoma Research*, 2015, 25(4): 284−294. https://doi.org/10.1097/CMR.0000000000000172

[3] W. Li, Y.H. Tian, Y. Liu, et al. Platycodin D exerts anti-tumor efficacy in H22 tumor-bearing mice via improving immune function and inducing apoptosis. *The Journal of Toxicological Sciences*, 2016, 41(3): 417−428. https://doi.org/10.2131/jts.41.417

[4] T. Wirth, N. Parker, S. Ylä-Herttuala. History of gene therapy. *Gene*, 2013, 525(2): 162−169. https://doi.org/10.1016/j.gene.2013.03.137

[5] H. Tian, J. Chen, X. Chen. Nanoparticles for gene delivery. *Small*, 2013, 9(12): 2034−2044. https://doi.org/10.1002/smll.201202485

[6] R. Mohammadinejad, A. Dehshahri, V.S. Madamsetty, et al. *In vivo* gene delivery mediated by non-viral vectors for cancer therapy. *Journal of Control. Release*, 2020, 325: 249−275. https://doi.org/10.1016/j.jconrel.2020.06.038

[7] N. Nayerossadat, T. Maedeh, P.A. Ali. Viral and nonviral delivery systems for gene delivery. *Advanced Biomedical Research*, 2012, 1: 27. https://doi.org/10.4103/2277-9175.98152

[8] Y.K. Sung, S.W. Kim. Recent advances in the development of gene delivery systems. *Biomaterials Research*, 2019, 23: 8. https://doi.org/10.1186/s40824-019-0156-z

[9] M. Ramamoorth, A. Narvekar. Non viral vectors in gene therapy- an overview. *Journal of Clinical and Diagnostic Research*, 2015, 9(1): GE01−GE06. https://doi.org/10.7860/JCDR/2015/10443.5394

[10] T. Wang, J.R. Upponi, V.P. Torchilin. Design of multifunctional non-viral gene vectors to overcome physiological barriers: Dilemmas and strategies. *International Journal of Pharmaceutics*, 2012, 427(1): 3−20. https://doi.org/10.1016/j.ijpharm.2011.07.013

[11] I. Khan, K. Saeed, I. Khan. Nanoparticles: Properties , applications and toxicities. *Arabian Journal of Chemistry*, 2019, 12(7): 908−931. https://doi.org/10.1016/j.arabjc.2017.05.011

[12] R.A. Saman, M. Iqbal. Nanotechnology-Based Drug Delivery Systems: Past , Present and Future. 2012: pp. 175–185.

[13] T.J. Harris, J.J. Green, P.W. Fung, et al. Tissue-specific gene delivery via nanoparticle coating. *Biomaterials*, 2010, 31(5): 998−1006. https://doi.org/10.1016/j.biomaterials.2009.10.012

[14] J. Zhao, G. Chen, X. Pang, et al. Calcium phosphate nanoneedle based gene delivery system for cancer genetic immunotherapy. *Biomaterials*, 2020, 250: 120072. https://doi.org/10.1016/j.biomaterials.2020.120072

[15] J. Buck, P. Grossen, P.R. Cullis, et al. Lipid-based DNA therapeutics: Hallmarks of non-viral gene delivery. *ACS Nano*, 2019, 13(4): 3754−3782. https://doi.org/10.1021/acsnano.8b07858

[16] F.L. Graham, A.J. van der Eb. A new technique for the assay of infectivity of human adenovirus 5 DNA. *Virology*, 1973, 52(2): 456−467. https://doi.org/10.1016/0042-6822(73)90341-3

[17] V. Sokolova, O. Prymak, W. Meyer-Zaika, et al. Synthesis and characterization of DNA-functionalized calcium phosphate nanoparticles. *Materwissenschaft und*

Werkstofftechnik, 2006, 37(6): 441−445. https://doi.org/ 10.1002/mawe.200600017

[18] R. Khalifehzadeh, H. Arami. Biodegradable calcium phosphate nanoparticles for cancer therapy. *Advances in Colloid and Interface Science*, 2020, 279: 102157. https:// doi.org/10.1016/j.cis.2020.102157

[19] M.A. Khan, V.M. Wu, S. Ghosh. Gene delivery using calcium phosphate nanoparticles: Optimization of the transfection process and the effects of citrate and poly(l-lysine) as additives. *Journal of Colloid and Interface Science*, 2016, 471: 48−58. https://doi.org/10.1016/j.jcis. 2016.03.007

[20] E.V. Giger, J. Puigmartí-Luis, R. Schlatter. Gene delivery with bisphosphonate-stabilized calcium phosphate nanoparticles. *Journal of Controlled Release*, 2011, 150(1): 87−93. https://doi.org/10.1016/j.jconrel.2010.11. 012

[21] V.L. Truong-Le, S.M. Walsh, E. Schweibert, et al. Gene transfer by DNA-gelatin nanospheres. *Archives of Biochemistry Biophysics*, 1999, 361(1): 47−56. https://doi. org/10.1006/abbi.1998.0975

[22] E.H. Chowdhury, T. Sasagawa, M. Nagaoka, et al. Transfecting mammalian cells by DNA/calcium phosphate precipitates: Effect of temperature and pH on precipitation. *Analytical Biochemistry*, 2003, 314(2): 316−318. https://doi.org/10.1016/S0003-2697(02)00648-6

[23] E.H. Chowdhury, M. Kunou, M. Nagaoka, et al. High-efficiency gene delivery for expression in mammalian cells by nanoprecipitates of Ca-Mg phosphate. *Gene*, 2004, 341: 77−82. https://doi.org/10.1016/j.gene.2004.07. 015

[24] G. Mancardi, C.E. Hernandez Tamargo, D. Di Tommaso, et al. Detection of Posner's clusters during calcium phosphate nucleation: A molecular dynamics study. *Journal of Materials Chemistry B*, 2017, 5(35): 7274−7284. https://doi.org/10.1039/c7tb01199g

[25] M. Banik, T. Basu. Calcium phosphate nanoparticles: A study of their synthesis, characterization and mode of interaction with salmon testis DNA. *Dalton Transactions*, 2014, 43(8): 3244−3259. https://doi.org/10.1039/c3dt 52522h

[26] J. Li, Y.C. Chen, Y.C. Tseng, et al. Biodegradable calcium phosphate nanoparticle with lipid coating for systemic siRNA delivery. *Journal of Controlled Release*, 2010, 142(3): 416−421. https://doi.org/10.1016/j.jconrel. 2009.11.008

[27] R. Khalifehzadeh, H. Arami. DNA-templated strontium-doped calcium phosphate nanoparticles for gene delivery in bone cells. *ACS Biomaterials Science & Engineering*, 2019, 5(7): 3201−3211. https://doi.org/10.1021/ acsbiomaterials.8b01587

[28] C.E. Pedraza, D.C. Bassett, M.D. McKee, et al. The importance of particle size and DNA condensation salt for calcium phosphate nanoparticle transfection. *Biomaterials*, 2008, 29(23): 3384−3392. https://doi.org/ 10.1016/j.biomaterials.2008.04.043

[29] C. Wu, J. Xu, Y. Hao, et al. Application of a lipid-coated hollow calcium phosphate nanoparticle in synergistic co-delivery of doxorubicin and paclitaxel for the treatment of human lung cancer A549 cells. *International Journal of Nanomedicine*, 2017, 12: 7979−7992. https://doi.org/10. 2147/IJN.S140957

[30] T. Welzel, I. Radtke, W. Meyer-Zaika, et al. Transfection of cells with custom-made calcium phosphatenanoparticles coated with DNA. *Journal of Materials Chemistry*, 2004, 14(14): 2213−2217. https:// doi.org/10.1039/B401644K

[31] V.V. Sokolova, I. Radtke, R. Heumann, et al. Effective transfection of cells with multi-shell calcium phosphate-DNA nanoparticles. *Biomaterials*, 2006, 27(16): 3147−3153. https://doi.org/10.1016/j.biomaterials.2005. 12.030

[32] C.M. Hoo, N. Starostin, P. West, et al. A comparison of atomic force microscopy (AFM) and dynamic light scattering (DLS) methods to characterize nanoparticle size distributions. *Journal of Nanoparticle Research*, 2008, 10: 89−96. https://doi.org/10.1007/s11051-008-9435-7

[33] Q.T.H. Shubhra, A. Oyane, H. Araki, et al. Calcium phosphate nanoparticles prepared from infusion fluids for stem cell transfection: Process optimization and cytotoxicity analysis. *Biomaterials Science*, 2017, 5(5): 972−981. https://doi.org/10.1039/c6bm00870d

[34] B. Sun, M. Gillard, Y. Wu, et al. Bisphosphonate stabilized calcium phosphate nanoparticles for effective delivery of plasmid DNA to macrophages. *ACS Applied Bio Materials*, 2020, 3(2): 986−996. https://doi.org/10. 1021/acsabm.9b00994

[35] A. Peetsch, C. Greulich, D. Braun, et al. Silver-doped calcium phosphate nanoparticles: Synthesis, characterization, and toxic effects toward mammalian and prokaryotic cells. *Colloids and Surfaces B*, *Biointerfaces*, 2013, 102: 724−729. https://doi.org/10.1016/j.colsurfb. 2012.09.040